

# UNRAVELING THE ROLE OF PRC1 AND 2 IN X INACTIVATION: A VALIDATION FOR THE USE OF EZH2 AND RING1B ANTIBODY IN ChIP

Robin van der Lee<sup>1,2</sup>, Bart Rooijackers<sup>1</sup> and Hendrik Marks<sup>1</sup>

<sup>1</sup>Department of Molecular Biology, Faculty of Science, Nijmegen Centre for Molecular Life Sciences (NCMLS), Radboud University Nijmegen, Nijmegen 6500 HB, The Netherlands; <sup>2</sup>Corresponding author. E-mail: r.vanderlee@student.ru.nl

---

Differentiation of female mouse and human ES cells triggers silencing of one X chromosome through X-chromosome inactivation (XCI). This process is required to equalize gene dosage between the sexes. After *Xist* RNA coats the inactive X chromosome (Xi), a series of epigenetic events occur that lead to silencing of the chromosome. However, the exact mechanisms behind this silencing process remain elusive. Disappearance of histone modifications associated with active chromatin and appearance of repressive marks like H3K27me3 and H2AK119ub are thought to be amongst the early steps of XCI. Following its *Xist*-mediated recruitment to the Xi, the Polycomb repressive complex 2 (PRC2) appears to be responsible for the trimethylation of H3K27. This mark in turn is believed to recruit PRC1, a complex with ubiquitin ligase activity specific for H2AK119. Eventually, these events result in incorporation of macroH2A and DNA methylation, leading to stable repression of the Xi. In order to further clarify the sequence of events during XCI, we here perform chromatin immunoprecipitation (ChIP) followed by quantitative PCR (qPCR; targeted ChIP) on chromatin obtained from cultured mouse embryonic stem (ES) cells and their differentiated derivatives. Using this approach, we validate the use of Ezh2 and Ring1B antibody in targeted ChIP. We detect colocalization of the PRC2-subunits Suz12 and Ezh2, and the PRC1-subunit Ring1B during all stages of differentiation at a selection of genes located across the whole mouse genome. These observations are consistent with the hypothesis that PRC2-mediated H3K27me3 deposition leads to PRC1 recruitment and eventually uH2A deposition. However, the results apply to a small subset of genes only, located across the whole genome and not specifically at the X chromosome.

---

## Introduction

In mammals, dosage of X-linked gene products is equalized between males and females by inactivation of one of the female X chromosomes [1]. During early female embryonic development in human and mice, random X inactivation of either the paternal or the maternal X takes place [2]. The formation of an inactive X chromosome involves a series of epigenetic changes, which include post-translational histone modifications and the recruitment of protein complexes responsible for their deposition (Fig. 1A) [3]. As a result of these series of repressive events, XCI provides a powerful model system to gain insights into the mechanisms of epigenetic gene repression. Initiation of the silencing process is regulated by the X-inactivation center (Xic), a region of approximately one Mb on the X chromosome [4]. The Xic encodes two non-coding RNAs, *Xist* and *Tsix*, whose coordinated expression determines which X will become inactivated. On the future inactive X (Xi), loss of *Tsix* expression permits

upregulation of *Xist* allowing for physical interaction between *Xist* RNA and the Xi in *cis* [5]. This is the basis of the inactivation process. In parallel, persistence of *Tsix* expression on the future active X (Xa) prevents upregulation of *Xist* thereby preventing silencing of both X chromosomes at once [6].

Information on epigenetic changes associated with XCI is widely based on immunofluorescence (IF) studies. The silent state of Xi is initially reversible and associated with a chromosome-wide loss of histone modifications associated with active chromatin [7]. Subsequently, the X chromosome undergoes trimethylation of histone H3 on lysine 27 (H3K27me3) [8,9] and H2A monoubiquitination (uH2A) [10], as well as enrichment of H3K9me2 and H4K20me1. The successive appearance of these histone modifications is proposed to underlie the progressive stability of the inactive state [11]. The Polycomb repressive complex 2 (PRC2), and in particular its methyltransferase subunit Ezh2, appears to be responsible for the deposition of

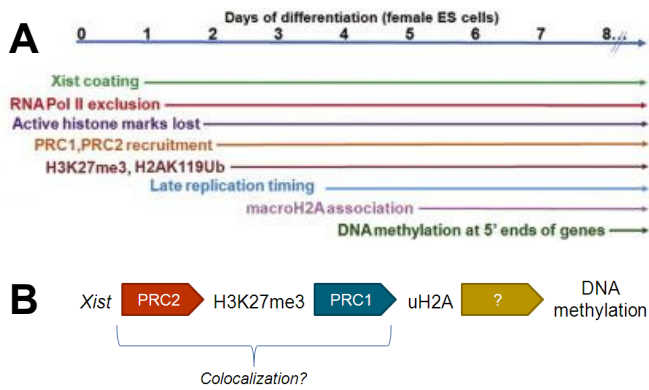


**Figure 1. (A)** Time range showing the cascade of events that lead from an initially reversible repression to a stably repressed inactive X chromosome during the differentiation of female embryonic stem cells. This data is based on immunofluorescence studies. Picture adapted and edited from Chow and Heard, 2009; *Current Opinion in Cell Biology*. **(B)** Xist-mediated recruitment of PRC2 is thought to lead to H3K27me3, which in turn recruits PRC1 leading to uH2A marks and further repressive events, like DNA methylation.

H3K27me3 and seems to be recruited to the Xi in a Xist RNA-dependent fashion (Fig. 1B) [8,9]. In turn, this mark is thought to allow for the recruitment of the PRC1 complex through interactions with its Cbx7 subunit [12]. The catalytic subunit of PRC1, Ring1B, is able to ubiquitinate histone H2A [13]. However, a recent study showed that PRC1 can also be recruited in a PRC2-independent way as Ring 1B is also recruited to the inactive X in PRC2-deficient cell lines [14]. Another complication rises from the fact that Polycomb complexes can be present in alternative compositions, as for instance the catalytic Ezh2 PRC2-subunit can be replaced by its Ezh1 counterpart [15]. The same holds for the PRC1 complex, which consists of four standard components that can all contain different proteins in different combinations, resulting in function redundancy. This variability makes it hard to study the Polycomb complexes by only their single subunits.

Later events during XCI include incorporation of macroH2A, a shift to late replication timing [16] and DNA methylation of promoters of X-linked genes. MacroH2A is enriched on the Xi in a cell-cycle dependent fashion from around day four onwards, but its role remains elusive [17]. DNA methylation, on the other hand, has clearly been shown to play an important role in stabilizing the inactive state of the Xi [18].

In order to further clarify the sequence of events leading to XCI, we here perform chromatin immunoprecipitation (ChIP) followed by

quantitative PCR (qPCR; targeted ChIP) on chromatin material from cultured mouse embryonic stem (ES) cells in different stages of differentiation. As these ES cells undergo XCI during differentiation, they provide a powerful system to study the process. We immunoprecipitate the Suz12 and Ezh2 PRC2-subunits and the catalytic PRC1 protein Ring1B and search for overlap between the binding sites of these proteins and available genome-wide H3K27me3 mouse ES cell profiles [19]. Moreover, we look at the kinetics of ChIP-qPCR recovery during differentiation for a small selection of genes located across the mouse genome. We also perform targeted ChIP against H2A ubiquitination. Using this approach, we validate the use Ezh2 and Ring1B antibody in targeted ChIP. We detect colocalization of the PRC2-subunits Suz12 and Ezh2, and the PRC1-subunit Ring1B during all stages of differentiation at a small selection of genes located across the whole mouse genome. When recoveries of one subunit decrease, recoveries of the others decrease as well. Furthermore we find that the enrichment of PRC1 and 2 on differentiation-specific genes usually decreases upon differentiation, with more enrichment present on genes in undifferentiated cells than in differentiated ones. These observations are consistent with the hypothesis that PRC2-mediated H3K27me3 deposition leads to PRC1 recruitment and eventually uH2A deposition. However, the results apply to a small subset of genes only, located across the whole genome and not specifically at the X chromosome.

## Results

In order to further examine the mechanisms of X-chromosome inactivation (XCI), several subunits of the PRC1 and PRC2 complexes were selected for investigation by chromatin immunoprecipitation (ChIP). For this purpose, we cultured female (LF2) and male (E14) mouse embryonic cells and harvested their chromatin from undifferentiated cells, 4-day atRA differentiated cells and 10-day Embryoid Bodies (EBs). Male ES cells are used to distinguish between epigenetic changes specific to XCI and changes occurring as a result of differentiation. However, since we merely performed ChIP-qPCR assays and therefore could not concentrate specifically on XCI by ChIP-seq and because of similarity between E14 and LF2 cells in pilot ChIP experiments, the E14 chromatin material was used only to validate early ChIP experiments and was no longer used in the

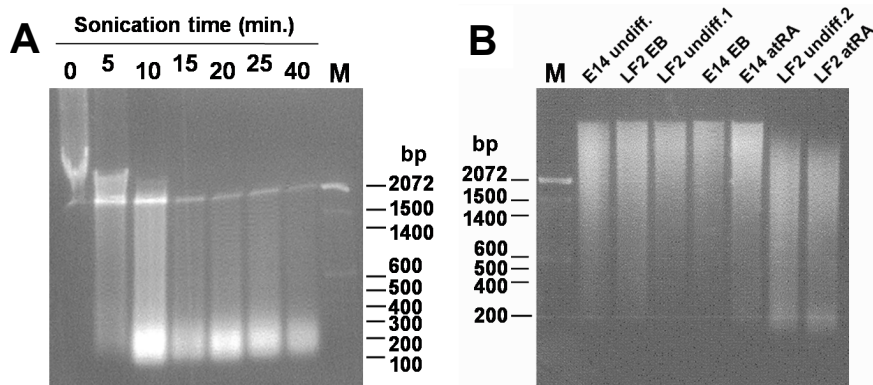


**Figure 2. (A)** Sonication time course on chromatin material from undifferentiated LF2 cells. At increasing times, aliquots of chromatin were withdrawn and DNA was purified. Then, equal amounts of DNA for each time point were size-separated on a 1% agarose gel in TBE and visualized with EtBr. Ten minutes of sonication produces fragmented DNA with a length between 100 and 2000 basepairs (bp), suitable for ChIP. **(B)** Chromatin material from LF2 and E14 cells and different stages of differentiation was sonicated for 13 minutes. A small amount was used to purify DNA and put on gel as described above. Undifferentiated LF2 chromatin (LF undiff.2) and 4d atRA differentiated LF2 chromatin (LF2 atRA) produced well-sized fragments with lengths varying between 100 and 2000 basepairs. The other chromatin samples were fragmented to a lower degree, creating larger fragments on average.

remaining experiments. ChIP-qPCR results are interpreted solely in terms of recovery compared to input sample. Occupancies, in which recovery values were normalized to recoveries of negative controls, were very similar and therefore not included.

### Fragmentation of chromatin material

Sonication was needed to fragment the harvested chromatin. A time course was performed with undifferentiated LF2 chromatin using an increasing sonication time range (0, 5, 10, 15, 20, 25, 40 min). After purification, the corresponding DNA was put on agarose gel (Fig. 2a). 10 minutes of sonication produced fragmented DNA with a length spread between 100 and 2000 basepairs, which is considered optimal for ChIP. Based on this experience, chromatin from LF2 and E14 ES cells was sonicated for 13 minutes and a small amount of DNA was put on gel to check the fragment size (Fig. 2b). One batch of undifferentiated LF2 chromatin (LF2 undiff.2) and the atRA LF2 chromatin produced the intended fragment size with lengths varying between 100 and 2000 basepairs. The other chromatin samples were less well fragmented, creating larger fragments on average. Therefore, chromatin samples used in later ChIP experiments were sonicated for 15 minutes.

For ChIPs performed using the anti-ubiquitinated H2A (uH2A) antibody,

mononucleosomal DNA fragments were created by a combination of sonication and micrococcal nuclease (MNase) treatment. In order to find out how long MNase digestion treatment was necessary to obtain mononucleosomal resolution, we carried out a time course with increasing amounts of digestion time. As a result, chromatin used in uH2A ChIP was sonicated for 15 minutes followed by a 25 minute MNase treatment. Attempts to put purified DNA on a gel to see if mononucleosomal resolution was obtained, failed.

### Antibody concentration

The concentrations of the monoclonal purified Ring1B and uH2A antibodies were obtained by measuring their absorption coefficient at 260 nm using a NanoDrop ND-1000

spectrophotometer. By means of a known BSA standard (supplementary figure 1), concentrations of the antibodies were calculated (Table 1). The concentrations of Ezh2 and Suz12 were not measured directly, since Ezh2 antibody is present in crude serum, which prevents correct measurements using the NanoDrop. Suz12 antibody concentration was provided by the supplier.

The optimal antibody concentration for Suz12 and uH2A for ChIPs were already known from previous experiments [20]. In order to find out how much Ezh2 and Ring1B antibody should be used in ChIP assays, an antibody concentration range with different amounts of antibody was performed using undifferentiated LF2 chromatin material. Real-time PCR results (supplementary figure 2) indicate the optimal amount of antibody for usage in ChIP (Table 1). We have hereby shown that chromatin immunoprecipitation assays can be

**Table 1.** Concentrations and amounts of antibodies used for ChIP

| Target | Concentration | Amount used in ChIP       |
|--------|---------------|---------------------------|
| Suz12  | 0.4 mg/ml     | 2 $\mu$ l (0.8 $\mu$ g)   |
| Ezh2   | -             | 3 $\mu$ l                 |
| Ring1B | 4.34 mg/ml    | 10 $\mu$ l (40.3 $\mu$ g) |
| uH2A   | 2.37 mg/ml    | 6.33 $\mu$ l (15 $\mu$ g) |

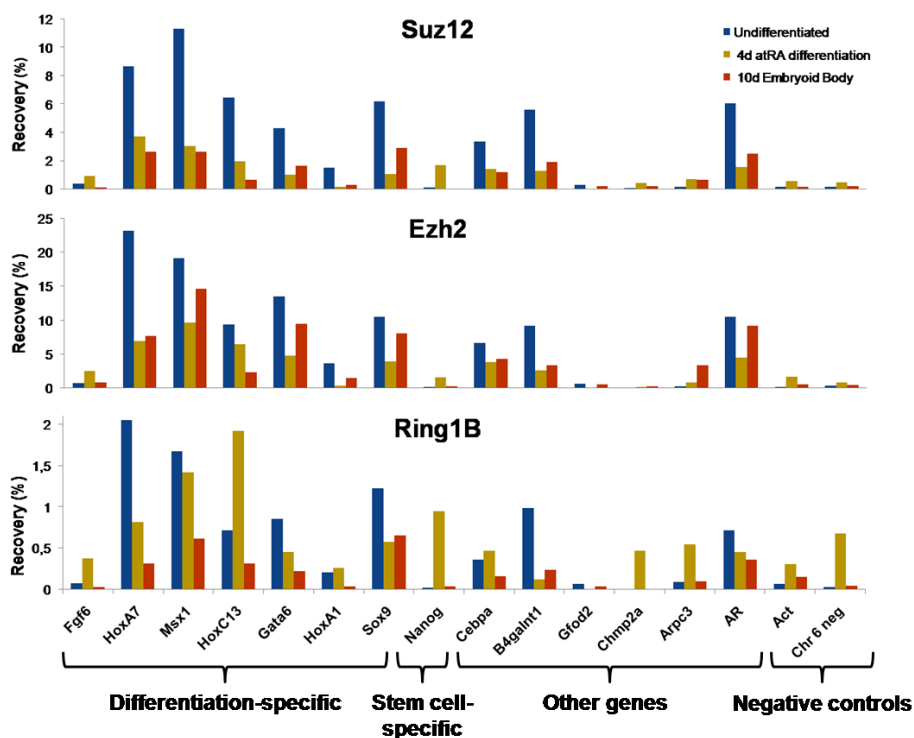


**Figure 3.** ChIP-qPCR results for antibodies against PRC2-subunits *Suz12* and *Ezh2*, and PRC1-subunit *Ring1B*. For each antibody, the percentage recovery of ChIPped material compared to input is shown for several differentiation-specific, stem cell-specific and other genes. *Actin* and a primer for chromosome 6 negative were used as negative controls. Results of all three antibodies show global similarities in terms of recoveries. Overall, each of these proteins seems to be present on the same genes roughly to the same extent, suggesting colocalization.

performed with *Ezh2* and *Ring1B* antibody and determined the optimal concentration of antibodies in ChIP.

### **Suz12, Ezh2 and Ring1B chromatin immunoprecipitation**

Chromatin immunoprecipitation with antibodies against PRC2-subunits *Suz12* and *Ezh2*, PRC1-subunit *Ring1B* and ubiquitinated H2A have been performed in combination with quantitative PCR. Primer pairs were designed to determine recoveries in differentiation-specific genes, stem cell-specific genes and other genes as well as primers where no recovery was expected (negative controls). *Suz12*, *Ezh2* and *Ring1B* qPCR results show global similarities (Fig. 3) in terms of the percentage recovery of ChIPped material compared to input. Overall, for the small selection of genes we analyzed, each of these proteins seems to be present on the same genes roughly to the same extent, suggesting colocalization. For example, differentiation-specific genes like *HoxA7*, *Msx1*, *HoxC13* and *Gata6* all show high recoveries for *Suz12*, *Ezh2* and *Ring1B*. In contrast, for *Fgf6*,

*HoxA1* and *Gfod2* far less to no recovery is observed for all three PRC-subunits.

Recovery of primers for differentiation-specific genes usually seems to decrease during differentiation, which can be expected as these genes usually will be activated during differentiation. This would involve disappearance of repressive chromatin marks like H3K27me3 and of the protein complexes presumably responsible for placing and maintaining repressive marks (like PRC1 and 2). The differentiation-specific primers clearly show higher recovery values than those of the negative controls such as *actin* and *chromosome 6 negative* (*chr 6 neg*). For the gene group termed 'other', recovery values vary significantly per gene. Especially *Cebpa* (CCAAT/enhancer binding protein alpha), *B4galnt1* (Beta-

14-N-acetyl galactosaminyltransferase) and

the androgen receptor gene (*AR*) show relatively high recoveries, whereas the remaining 'other' genes show little ChIP recovery as compared to input material.

Two trends can be found most often in the ChIP-qPCR results for all three antibodies. First, a tendency in which we find a high recovery in undifferentiated cell material compared to a low one in 10d Embryoid Body material. The other shows a different development, with 4d atRA sample showing the lowest recovery flanked by higher undifferentiated and Embryoid Body values. In both trends however, undifferentiated chromatin shows the highest recovery. Variations between different chromatin samples can be seen as well, such as the high overall recovery rate of chromatin of 4 days differentiated cells immunoprecipitated with *Ring1B* antibody. The *Ezh2* antibody delivers relatively lower recoveries with atRA material, but its EB recoveries are high compared to *Ring1B* and *Suz12* ChIPs. Given the variable results, the essential observation of both trends seems to be the fact that recoveries drop with differentiation, which often correlates with differentiation-specific genes.

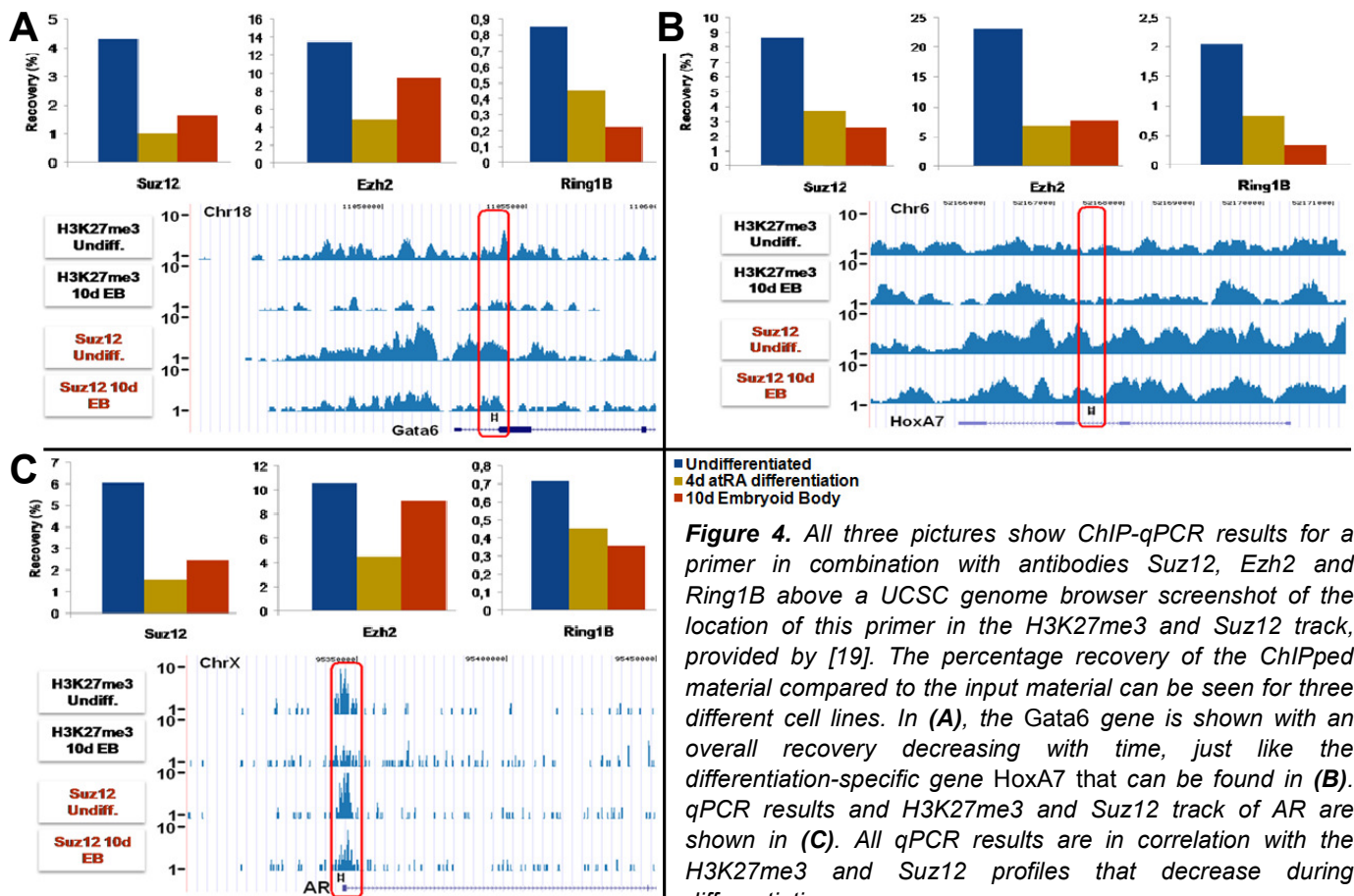


**Figure 4.** All three pictures show ChIP-qPCR results for a primer in combination with antibodies Suz12, Ezh2 and Ring1B above a UCSC genome browser screenshot of the location of this primer in the H3K27me3 and Suz12 track, provided by [19]. The percentage recovery of the ChIPped material compared to the input material can be seen for three different cell lines. In (A), the Gata6 gene is shown with an overall recovery decreasing with time, just like the differentiation-specific gene HoxA7 that can be found in (B). qPCR results and H3K27me3 and Suz12 track of AR are shown in (C). All qPCR results are in correlation with the H3K27me3 and Suz12 profiles that decrease during differentiation.

When recovery values are compared between the different antibodies, Ezh2 antibody stands out with recoveries up to 20%, whereas Suz12 gives recoveries only half these values. The Ring1B antibody shows the lowest recoveries, having values between 1% and 2%. This study shows that the Suz12, Ezh2 and Ring1B antibodies do work in ChIP.

### qPCR comparison with genome-wide H3K27me3 and Suz12 profiles

Genome-wide H3K27me3 and Suz12 profiles have been produced using ChIP-seq by previous studies with mouse ES cells [19]. We compared our qPCR results with these profiles. Figures 4a-c show the Suz12, Ezh2 and Ring1B recoveries of HoxA7, Gata6 and AR together with the K27 trimethylation and Suz12 landscape surrounding these genes. HoxA7 (Fig. 4a) exhibits decreasing recoveries for each antibody during differentiation. This tendency is expected for differentiation-specific genes and corresponds with both the H3K27me3 and the Suz12 profile over HoxA7: in undifferentiated ES cells, there is more trimethylation of H3K27 and more binding of Suz12 than in 10-day differentiated EBs.

Similar same profiles are present for the Gata6 gene. Recovery kinetics as measured with qPCR however (Fig. 4b) differ slightly from those of HoxA7, with the atRA chromatin having the lowest recovery for Suz12 and Ezh2 ChIPs, and a decreasing trend for Ring1B. The Androgen Receptor (AR) gene is located on the X chromosome. The available profiles show a large peak of both H3K27me3 and Suz12 at the promoter of AR (Fig.4c). Once again there is a decrease of H3K27me3 deposition and Suz12 presence during differentiation. A similar decrease for the presence of Ring1B as well as Ezh2 is shown by qPCR, yet to a smaller extent.

### uH2A chromatin immunoprecipitation

Next to ChIPs against Polycomb complex subunits, a ChIP has been performed with an antibody against monoubiquitinated H2A. In order to obtain quality results, we adjusted the chromatin harvest procedure by means of including micrococcal nuclease digestion and nuclease isolation, according to [20]. However, qPCR recovery values remain very low although there are exceptions (Fig. 5a). Recoveries in 4d atRA differentiated cells are very high in comparison to undifferentiated and

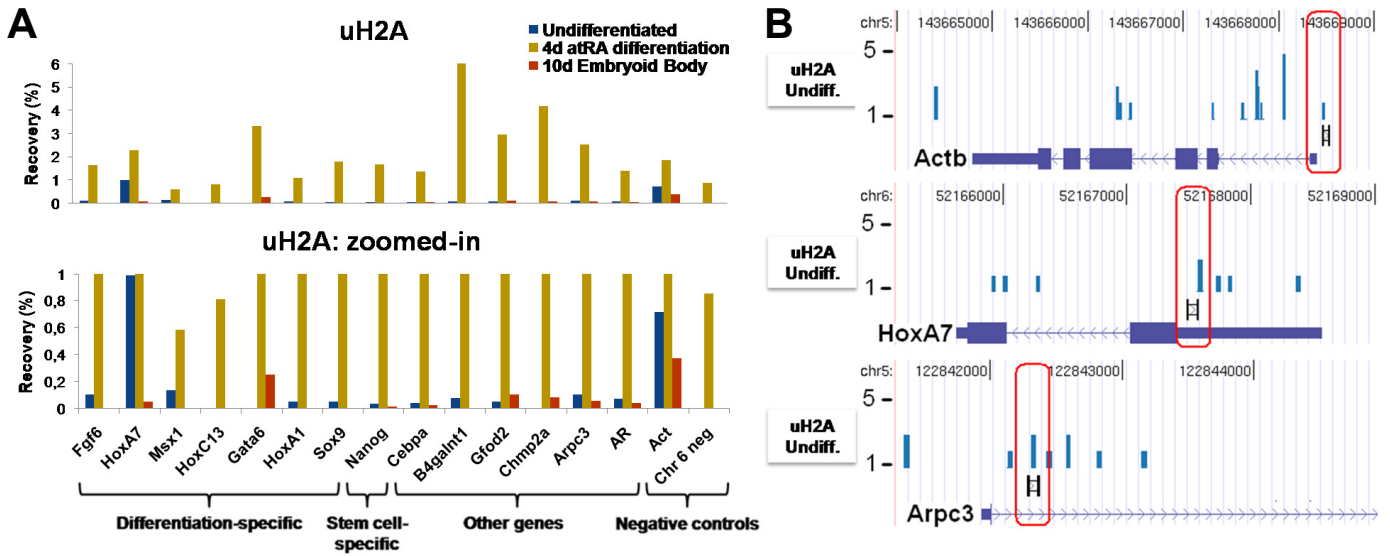


**Figure 5. (A)** ChIP-qPCR results for ubiquitinated H2A. The percentage recovery of ChIPped material compared to input is shown for the same primers as used before. Overall, recovery values remain low, with the exception of 4d atRA differentiated cells. The zoomed-in graph gives a better view on the relative differences between undifferentiated and 10d Embryoid Body material. **(B)** Screenshots from the UCSC genome browser showing the distribution of the uH2A ChIP-seq profile from [20] across the Actin, HoxA7 and Arpc3 genes (UCSC Mouse [mm9], July 2007) in mouse embryonic fibroblast cells. The profiles show low ubiquitination genome-wide and across these genes in particular, corresponding with the minor recoveries of uH2A at the location of the primers in figure A.

10d EB material, especially on the *B4galnt1* gene. Given these results it seems that ChIP using the uH2A antibody is not fully optimized yet. But because genome wide ChIP-seq uH2A profiles of mouse embryonic fibroblasts [20] show low ubiquitination genome-wide, the low values as observed with qPCR could just as well be a reflection of the *in vivo* situation. In figure 5b, the profiles showing the surroundings of *Actin*, *HoxA7* and *Arpc3* are given. All three show relatively high recovery values for undifferentiated and 10d Embryoid Body cells as compared to other genes. Their surrounding uH2A profiles correspond with the still minor recovery of uH2A at the location of the primers.

## Discussion

We performed chromatin immunoprecipitation studies with several antibodies to gain more insight in the cascade of events leading to X-chromosome inactivation. Antibodies against subunits Ezh2 and Suz12 (Polycomb repressive complex 2, PRC2) and Ring1B (PRC1) have been examined and showed similar results. Enrichments are overall alike, although absolute recovery values differ, with Ezh2 showing the highest recovery followed by Suz12 and Ring1B. Recoveries of these protein decrease during differentiation, especially with

differentiation-specific genes like *HoxA7* and *Gata6*, which is in line with expectations.

## Variation in ChIP results

When we evaluate the ChIP results, some peculiarities can be noticed and the results were not always reproducible. atRA recovery values seem to differ with different antibodies, being relatively higher in combination with the Ring1B antibody as well as the uH2A antibody. The Embryoid Body LF2 and undifferentiated LF2 show very low recovery values in the uH2A ChIP. These differences could be caused by the quality of the chromatin used. In order to test chromatin quality and correct for the dissimilarities between several chromatin samples, an additional negative control could be added in future experiments, like mock-experiments lacking only antibody. Suz12 has proven to be a good ChIP-grade antibody and could function as a control for chromatin quality too. To check if the remaining variation has biological causes, replication of the data is necessary.

Since Embryoid Bodies are already ten days into differentiation, differences in gene expression and epigenetic landscapes between cells are likely to be present as compared to undifferentiated cells. Therefore, chromatin of these cells is likely to show varying recovery values. This might be the

cause of the relatively high recoveries seen with EB material in Ezh2 ChIPs in our results.

The extreme variation found in its qPCR results show that the ChIP with uH2A antibody is not very efficient and that the protocol might have to be optimized, although enrichments in a ChIP-Seq experiment of uH2A were very low as well [20].

### **Colocalization of PRC1, PRC2 and H3K27me3**

Recently it was reported that PRC1, besides the previously known PRC2-dependent way, can also be recruited to the chromosome in a PRC2-independent way [14]. In this study, we find colocalization between the PRC2 subunits, Suz12 and Ezh2, and the Ring1B PRC1 subunit on all genes we looked at. Furthermore, these enrichments also colocalize with H3K27me3. We found no genes at which only PRC1 or PRC2 is enriched. This suggests that, at least for the genes that we analyzed, PRC1 is recruited in a PRC2-dependent manner only. This presumably happens as a result of an interaction between PRC1 and the H3K27me3 mark deposited by PRC2.

The Polycomb complexes can be present in alternative combinations, as reported in [15]. This property questions the use of specific antibodies as representatives for the whole corresponding complex. In the case of PRC2, there is less redundancy than for PRC1 (see supplementary Fig. 3). The use of Suz12 to represent PRC2 seems justified, since there are no other proteins that can take over of the role of this protein. The catalytic function is usually represented by Ezh2, but can occasionally be replaced by Ezh1. However, since we studied both Suz12 and Ezh2, it seems likely that genes at which these proteins colocalize are indeed bound by PRC2. For PRC1, many more subunit combinations are possible and therefore we looked at the subunit responsible for the catalytic ubiquitin ligase activity, Ring1B. This subunit is necessary for the activity of the complex so it seems likely that we studied the core of the complex. Therefore, the observed colocalization between Suz12, Ezh2 and Ring1B is likely to be real, supporting the hypothesis that PRC2-mediated H3K27me3 deposition leads to PRC1 recruitment and eventually uH2A deposition.

However, since our experiments do not focus on the X chromosome, they are not sufficient to conclude whether colocalization of the PRC subunits occurs genome-wide or as part of the XCI. Also, since replicate experiments have not been performed, reproduction of the data is necessary to further support the hypothesis that

PRC2-mediated H3K27me3 deposition leads to PRC1 recruitment.

### **Future research**

In our research, we intended to investigate XCI which serves as a model system for epigenetic regulation of gene repression. To unravel more about XCI, the next step is the use of next generation sequencing to perform ChIP-seq with the antibodies we validated using ChIP-qPCR. ChIP-seq delivers high resolution data leading to more extensive and solid conclusions. Profiles obtained by this approach can be compared with previously available profiles, leading to knowledge about the sequence of events during XCI. For the uH2A antibody, ChIP protocol should be optimized after which further validation and deep sequencing can be applied. Additionally, because PRC1 (and PRC2 to a lesser extent) has several appearances existing of different subunits with the same activity, different subunits should be ChIPped and sequenced as well to get full coverage of PRC1 binding sites and to find out the exact working mechanism of these enzymes.

### **Methods**

*Additional protocols can be found in the supplementary information.*

#### **E14 and LF2 cell culture**

Female LF2 and male E14 mouse embryonic stem cells were cultured (thawing, passaging, expansion and freezing) based on the previously described standard protocols of the Wellcome Trust Sanger Institute (<http://www.sanger.ac.uk/PostGenomics/genetrap/protocols/GeneralInformation.pdf>).

Stem cell differentiation using four day all-trans-retinoic acid (atRA) treatment was performed based on [21]: 80% confluent cell plates were washed twice with PBS and trypsinized. Trypsin was neutralized using cell culture medium containing anti-differentiation factors. After counting using a Coulter AC T Series Analyzer, the cells were plated at a density of  $2 \times 10^4$  cells/cm<sup>2</sup> and grown like undifferentiating stem cells for one day (using LIF-containing medium). Then, the cells were rinsed thoroughly of LIF by washing them three times with PBS. Next, medium without LIF was added together with  $10^{-6}$  M atRA. During differentiation, the medium with retinoic acid was changed daily. atRA concentration was adjusted according to the observed ratio of cell death and differentiation.

For Embryoid Body formation (ten days), confluent cell plates were washed with PBS and trypsinized using a low concentration of trypsin for two minutes at room temperature. Deattached cells were made sure to remain in clumps. The obtained cell suspension was divided over multiple non-gelatin coated bacterial dished

using a glass pipet with wide opening. Cells were grown in clumps for two days and attachment was prevented by swirling them around every day. On day three, the swimming Embryoid Bodies were placed in gelatin coated plates using a pipet with wide opening. Medium was changed daily.

### Antibodies

The concentration of the Ring1B and uH2A antibodies was measured using the NanoDrop ND-1000 spectrophotometer with BSA correlation. Suz12 antibody concentration was provided by Abcam. Ezh2 could not be measured correctly since this antibody is present in none-purified serum (Table 2).

### Chromatin harvest and fragmentation

Methods for the harvest and fragmentation of chromatin material differ between samples meant for uH2A ChIP and samples meant for ChIP with Suz12, Ezh2 and Ring1B. A combination of the protocols used for Suz12, Ezh2 and Ring1B chromatin immunoprecipitation and the protocol used in [20] led to the procedure for uH2A ChIP.

#### Suz12, Ezh2 and Ring1B

Cells were trypsinized and dissolved in medium to a concentration of  $5 \times 10^6$  cells/ml. 1% formaldehyde was added and the solution was rotated at room temperature for 30 minutes to crosslink the cells. The reaction was stopped by adding 125 mM glycine, resulting in a yellow colored solution [23]. Cells were washed with cold PBS and several buffers by ten minutes rotation at four degrees centigrade. Sample pellet was dissolved in ChIP incubation buffer containing protease inhibitors to a concentration of  $33 \times 10^6$  cells/ml.

Chromatin samples were sonicated into fragments with an average length of 0.5 to 2 kilobases. The required time for sonication was determined using a timecourse and fragment length analysis on agarose gel after de-crosslinking and DNA isolation. After 13 minutes (decided to be the optimal duration) of sonication, the samples were centrifuged to get rid of cellular debris.

#### uH2A

After trypsinization and crosslinking as described above, the cells were washed twice with PBS. The cells were resuspended in one volume of cell lysis buffer and kept on ice for ten minutes. In order to isolate nuclei, one volume of Solution B was added.

Next, the chromatin was sonicated for 15 minutes to obtain an average fragment length of 0.5–2 kb and the

cellular debris was removed by spinning it down. Micrococcal digestion was then performed with the purpose of acquiring mononucleosomal fragment resolution. In order to gain insight in how long digestion (MNase) treatment was necessary, a timecourse was first carried out. Sonicated chromatin was treated with 0.06 units of micrococcal nuclease per  $\mu\text{g}$  chromatin (as measured using the NanoDrop ND-1000 spectrophotometer) for 25 minutes (decided to be the optimal treatment duration) at  $37^\circ\text{C}$ . To stop the reaction, 10 mM of EDTA was added, followed by one volume of modified lysis buffer. In order to determine fragment size of each sample after sonication and, for uH2A samples, after sonication and digestion, part of the fragmented chromatin was de-crosslinked and the corresponding DNA isolated to put on gel.

### ChIP

Immunoprecipitation was carried out using protein-A Sepharose bead. After swelling the beads in PBS, they were blocked for aspecific binding by washing twice and incubating for 2 hours at  $4^\circ\text{C}$  with 0.1% bovine serum albumin (BSA) in incubation buffer. IP mixtures (beads, fragmented chromatin and antibody amongst other components) were incubated by overnight rotation at  $4^\circ\text{C}$  and washed with several buffers afterwards. Then, using elution buffer with a high salt concentration, immunoprecipitated chromatin was eluted from the beads followed by addition of  $16 \mu\text{l}$  5M NaCl to the supernatant. De-crosslinking was done by shaking the samples for 5 hours at  $65^\circ\text{C}$ . Next, DNA was isolated using Phenol Chloroform Isoamyl alcohol (PCI) extraction, followed by precipitation at  $-20^\circ\text{C}$  using 100% ethanol, glycogen and NaAc. Input DNA sample was prepared by de-crosslinking fragmented chromatin, followed by DNA isolation.

### qPCR

For a list of primers used in qPCR analysis of ChIPs, see supplementary information. BioRad SYBR Green Supermix was used to detect and measure real-time changes in DNA concentration during the polymerase chain reaction. A two step and melt protocol was used on BioRad MyiQ qPCR machines.

Analysis of qPCR results were carried out using the BioRad iQ5 program. Melting curves of each well were checked on the presence of only a PCR single product. Then, an appropriate fluorescent detection threshold was determined. The corresponding cycles were analyzed using Excel. ChIP data was represented as percentage recovery compared to input sample using the following formula: Recovery =  $2^{\Delta C_T}$  (## cycles IP

**Table 2.** Antibody information

| Target | Antibody #                | Antibody lot | Type        | Supplier      | Concentration | Amount used in ChIP                    |
|--------|---------------------------|--------------|-------------|---------------|---------------|--|
| Suz12  | ab12073-100               | 418328       | Polyclonal  | Abcam         | 0.4 mg/ml     | 2 $\mu\text{l}$ (0.8 $\mu\text{g}$ )   |
| Ezh2   | 05-678                    | -            | Crude serum | Active Motif  | -             | 3 $\mu\text{l}$                        |
| Ring1B | Koseki et al. (2001) [22] |              | Monoclonal  | Koseki et al. | 4.34 mg/ml    | 10 $\mu\text{l}$ (40.3 $\mu\text{g}$ ) |
| uH2A   | 05-678 (E6C5)             | DAM1588211   | Monoclonal  | Millipore     | 2.37 mg/ml    | 6.33 $\mu\text{l}$ (15 $\mu\text{g}$ ) |

sample - # cycles input sample) \*correction factor). The correction factor represents the difference in the original amount of chromatin used for template and IP samples as well as the different fold dilutions of the isolated DNA. According to the recovery graphs generated on this way, a robust background primer pair was chosen. In order to get occupancy graphs, recovery values were then divided by those of the background primer pair for each sample. These graphs represent fold changes over background.

### Primers

uH2A-specific primers were designed using genome-wide H3K27me3 and Suz12 profiles (unpublished data, available at <http://mb01.azn.nl/~hendrik/Edith/>) as well as a recently published uH2A profile in MEF-cells ([20].

available at <http://www.ncbi.nlm.nih.gov/projects/geo/query/acc.cgi?acc=GSE15909>), which was converted from mm8 mouse genome build to mm9 using the 'Batch Coordinate Conversion (liftOver)' from the UCSC Genome Browser [24]. This browser was used to view these profiles as well. As uH2A is supposed to be present preferentially at gene transcription start sites (TSS) [25], some genes with robust H3K27 methylation and Suz12 enrichment at the TSS were chosen to design primers against. Also, [25,26] showed genes at which uH2A is present at specific spots around the TSS. These genes, HoxC13 and HoxA7 respectively, were chosen as primer targets as well. For a full list of primers with their corresponding genome locations and targets, see the supplementary information.

### References

- [1] Lyon, M.F. (1961). Gene action in the X chromosome of the mouse (*Mus musculus* L.). *Nature* **190**: 372–373.
- [2] Okamoto I , Otte AP , Allis CD , Reinberg D , Heard E (2004) Epigenetic dynamics of imprinted X inactivation during early mouse development. *Science* **303**: 644–649.
- [3] Edith Heard and Christine M. Disteche (2006). Dosage compensation in mammals: fine-tuning the expression of the X chromosome. *Genes Dev.* **20**: 1848-1867.
- [4] Heard E, Avner P. (1994). Role play in X-inactivation. *Hum Mol Genet* **3**: 1481–1485.
- [5] C. Clemson, J.A. McNeil, H.F. Willard and J.B. Lawrence, XIST RNA paints the inactive X chromosome at interphase: evidence for a novel RNA involved in nuclear/chromosome structure, *J Cell Biol* **132** (1996); 259–275.
- [6] J.T. Lee et al. (1999). Tsix, a gene antisense to Xist at the X-inactivation centre, *Nat Genet* **21**: 400–404.
- [7] Heard, E., Rougeulle, C., Arnaud, D., Avner, P., Allis, C.D., and Spector, D.L. (2001). Methylation of histone H3 at Lys-9 is an early mark on the X chromosome during X-inactivation. *Cell* **107**: 727.
- [8] Plath K , Fang J , Mlynarczyk-Evans SK , Cao R , Worringer KA , Wang H , de la Cruz CC , Otte AP , Panning B , Zhang Y (2003). Role of histone H3 lysine 27 methylation in X inactivation. *Science* **300**: 131–135.
- [9] Silva J , Mak W , Zvetkova I , Appanah R , Nesterova TB , Webster Z , Peters AH , Jenuwein T , Otte AP , Brockdorff N (2003) Establishment of histone h3 methylation on the inactive X chromosome requires transient recruitment of Eed-Enx1 polycomb group complexes. *Dev Cell* **4**: 481–495.
- [10] de Napoles M , Mermoud JE , Wakao R , Tang YA , Endoh M , Appanah R , Nesterova TB , Silva J , Otte AP , Vidal M , Koseki H , Brockdorff N (2004) Polycomb group proteins Ring1A/B link ubiquitylation of histone H2A to heritable gene silencing and X inactivation. *Dev Cell* **7**: 663–676.
- [11] Kohlmaier A , Savarese F , Lachner M , Martens J , Jenuwein T , Wutz A (2004). A chromosomal memory triggered by *Xist* regulates histone methylation in X inactivation. *PLoS Biol* **2**: E171.
- [12] Bernstein et al. (2006). Mouse Polycomb Proteins Bind Differentially to Methylated Histone H3 and RNA and Are Enriched in Facultative Heterochromatin. *Molecular and cellular biology* **26**: 2560-2569.
- [13] Wang H, Wang L et al. (2004). Role of histone H2A ubiquitination in Polycomb silencing. *Nature* **431** (7010):873-8.
- [14] Schoeftner S, Sengupta AK, Kubicek S, Mechtler K, Spahn L, Koseki H, Jenuwein T, Wutz A (2006). Recruitment of PRC1 function at the initiation of X inactivation independent of PRC2 and silencing. *EMBO J* **25**: 3110–3122.
- [15] Lena Ho, Gerald R. Crabtree (2008). An EZ Mark to Miss. *Cell Stem Cell* **3** (6): 577-578.
- [16] Takagi N, Sugawara O, Sasaki M. (1982). Regional and temporal changes in the pattern of X-chromosome replication during the early postimplantation development of the female mouse. *Chromosoma* **85**: 275–286.
- [17] Constanzi, C., Stein, P., Worrad, D.M., Schultz, R.M., and Pehrson, J.R. (2000). Histone macroH2A1 is concentrated in the inactive X chromosome of female preimplantation mouse embryos. *Development* **127**: 2283.
- [18] Heard, E., Clerc, P., and Avner, P. (1997). X chromosome inactivation in mammals. *Annu. Rev. Genet.* **31**: 571.
- [19] High-resolution analysis of epigenetic changes associated with X inactivation (2009). Hendrik Marks, Jennifer C. Chow, Sergey Denissov, Kees-Jan Francxiojs, Neil Brockdorff, Edith Heard and Hendrik G. Stunnenberg. *Genome Research*.
- [20] Kallin EM, Cao R, Jothi R, Xia K, Cui K, et al. (2009). Genome-Wide uH2A Localization Analysis Highlights Bmi1-Dependent Deposition of the Mark at Repressed Genes. *PLoS Genet* **5**(6): e1000506. doi:10.1371/journal.pgen.1000506.
- [21] Smith, A. G. J. (1991). *Tiss. Cult. Meth.* **13**: 89–94 .
- [22] Tomonori Atsuta, Shuichi Fujimura, Hideshige Moriya, Miguel Vidal, Takeshi Akasaka, Haruhiko Koseki (2001). Production of Monoclonal Antibodies Against Mammalian Ring1B Proteins. *Hybridoma* **20**(1): 43-46..
- [23] Valerio Orlando, Helen Strutt, and Renato Paro (1997). Analysis of Chromatin Structure by in Vivo Formaldehyde Cross-Linking. *Enzymology* **11**: 205–214.
- [24] Kent WJ, Sugnet CW, Furey TS, Roskin KM, Pringle TH, Zahler AM, Haussler D (2002). The human genome browser at UCSC. *Genome Res.* **12**(6):996-1006.
- [25] R. Cao, et al. (2005). Role of Bmi-1 and Ring1A in H2A Ubiquitylation and Hox Gene Silencing. *Molecular Cell* **20**: 845-854.
- [26] Wu X, Gong Y, Yue J, Qiang B, Yuan J, Peng X (2008). Cooperation between EZH2, NSPc1-mediated histone H2A ubiquitination and Dnmt1 in HOX gene silencing. *Nucleic Acids Res.* **36**(11):3590-9.